NUREG/CR-0145
ORNL/NUREG/TM-207

Noise Diagnostics for Safety Assessment, Standards, and Regulation Quarterly Progress Report for January–March 1978

D. N. Fry
R. C. Kryter
J. E. Stoneking
F. J. Sweeney

Prepared for the U.S. Nuclear Regulatory Commission
Office of Nuclear Regulatory Research
Under Interagency Agreements DOE 40-551-75 and 40-552-75

OAK RIDGE NATIONAL LABORATORY
OPERATED BY UNION CARBIDE CORPORATION · FOR THE DEPARTMENT OF ENERGY

Printed in the United States of America. Available from
National Technical Information Service
U.S. Department of Commerce
5285 Port Royal Road, Springfield, Virginia 22161

NUREG/CR-0145
ORNL/NUREG/TM-207
Dist. Category R1

Contract No. W-7405-eng-26

INSTRUMENTATION AND CONTROLS DIVISION

NOISE DIAGNOSTICS FOR SAFETY ASSESSMENT, STANDARDS, AND REGULATION
QUARTERLY PROGRESS REPORT FOR JANUARY-MARCH 1978

D. N. Fry, R. C. Kryter, J. E. Stoneking, and F. J. Sweeney

Manuscript Completed — May 9, 1978

Date Published — June, 1978

NOTICE: This document contains information of preliminary nature. It is subject to revision or correction and therefore does not represent a final report.

Prepared for the
U.S. Nuclear Regulatory Commission
Offices of Nuclear Regulatory Research,
Nuclear Reactor Regulation, and Standards Development
Washington, D. C. 20555
Under Interagency Agreements DOE 40-551-75 and 40-552-75

NRC FIN Nos. B0092, B0723, and B0191

Prepared by the
OAK RIDGE NATIONAL LABORATORY
Oak Ridge, Tennessee 37830
operated by
UNION CARBIDE CORPORATION
for the
DEPARTMENT OF ENERGY

ABSTRACT

Progress, numerical results, and interim conclusions are reported in three work areas funded by NRC: surveillance success predictive modeling, screening techniques for vibrational qualification of nuclear plant piping, and evaluation of BWR-4 bypass flow modifications through study of associated changes in the in-core neutron noise signals.

CONTENTS

1. SCOPE OF PROGRESS REPORT

Beginning with this report, covering the second quarter of FY 1978, the scope will be expanded to include selected work in progress under ORNL 189a Nos. B0191, B0092, and B0723, which are supported by the Offices of Nuclear Regulatory Research (Division of Reactor Safety Research), Nuclear Reactor Regulation (Division of Operating Reactors), and Standards Development (Division of Engineering Standards), respectively. Since, in many instances, the work is performed under a cost-sharing arrangement among the Divisions, we have chosen not to single out a "sponsor" for each task. These quarterly progress reports will emphasize numerical results, interim conclusions, and, as desirable, details of the scientific method employed. Most often, an understanding of the general nature, scope, task goals, and reasons for undertaking the work will be either presumed or stated in the most brief terms, and purely descriptive background information will ordinarily be omitted. The reader desiring a more general description of the total work in progress and the accomplishments to date is referred to the bimonthly informal activities reports.

This quarter's report highlights three work areas: surveillance success predictive modeling, screening techniques for qualifying plant piping against excessive levels of vibration, and highly automated data handling and display techniques for use in relating changes in BWR-4 in-core neutron noise signals to bypass flow modifications that have been effected to correct excessive vibration of instrument tubes.

2. SURVEILLANCE SUCCESS PREDICTIVE MODELING

F. J. Sweeney

Purpose. Determine the sensitivity for the detection and quantification of anomalous in-vessel noise sources that might be provided by noise analysis of signals from installed sensors.

Method. Construction of noise-equivalent sources (Langevin technique).

First Application. Void in BWR fuel channel, as sensed by in-core neutron detectors.

Follow-on. Control rod, fuel element, and structural vibrations.

2.1 Introduction

In a BWR a principal fluctuating quantity of interest is the void fraction. By constructing a suitable model for two-phase flow, fluctuations in the void fraction and steady-state operating characteristics can be interrelated. Such a model can also be utilized to predict void fraction fluctuations resulting from an anomalous condition, such as internals vibration or flow blockage.

After the two-phase flow patterns have been modeled, the next step is to relate fluctuations of the void fraction to the resultant perturbations of the neutron detector signals. A spatial transfer function or a variational technique is needed to relate the void fluctuations at different locations in the fuel bundles to the detector fluctuations that they produce. Thus, modeling BWR neutron noise requires the development of both a two-phase flow model and a variational technique or spatial transfer function. In the following text, only the development and results of an analytical, two-phase flow model will be discussed; for a discussion of the development of a variational technique, see Ref. 1.

2.2 Development of an Analytical Model for Two-Phase Flow

A model for two-phase flow can be developed by employing either analytical or numerical techniques to solve the linearized continuity equations. The advantage of the analytical technique is that the input variables can be parametrically excited and the resulting effects on the quantity of interest can be observed. Its principal disadvantage is that the simplifying assumptions usually necessary to obtain an analytical solution may restrict the applicability of the results to actual conditions. For BWRs, we believe that the advantages of the analytical technique outweigh its disadvantages, at least as a method for studying the important question of whether the noise sources that

drive the void fraction fluctuations are axially correlated or uncorrelated; hence, we have used the analytical method exclusively in obtaining the results discussed in this report.

Finally, we acknowledge that while other researchers[2,3] have developed two-phase flow models, their models have failed to predict correctly the resulting detector fluctuations. Thus, valid two-phase flow models alone will not predict neutron detector fluctuations; the model must be combined with an accurate spatial transfer function or a variational technique.

2.3 Initial Results from Analytical Investigations

The analytical solutions discussed here were obtained by the method described by Williams[4] and Akcasu.[5] Figures 1 and 2 show the magnitude of the cross-power spectral density, |CPSD|, and the relative phase between local void fluctuations at 18 in. and at 54 in. from the bottom of a typical BWR fuel bundle, as predicted by our analytical two-phase flow model. Likewise, Figs. 3 and 4 illustrate the predicted |CPSD| and phase functions of void fluctuations at 90-in. and 126-in. axial positions. These CPSDs result from summing the results from 16 simulated subchannels within the fuel bundle. To obtain these results we assumed initially that the driving noise sources were axially *uncorrelated*. Several observations were made:

1. The phase is approximately a linear function of frequency from 0 to 25 Hz;
2. The steam velocity between the 18- and 54-in. levels, as derived from the phase vs frequency curve, is ∿12 ft/sec, whereas between the 90- and 126-in. levels it is ∿33 ft/sec;
3. The magnitude of the CPSD increases with increased distance from the bottom of the bundle.

These observations agree with experimental data from operating BWRs.[6] In contrast, when axially *correlated* driving functions were assumed, our model predicted void fluctuation spectra with phase functions that oscillated around zero and hence yielded no consistent steam velocity. Such predictions clearly disagree with experimental observation,

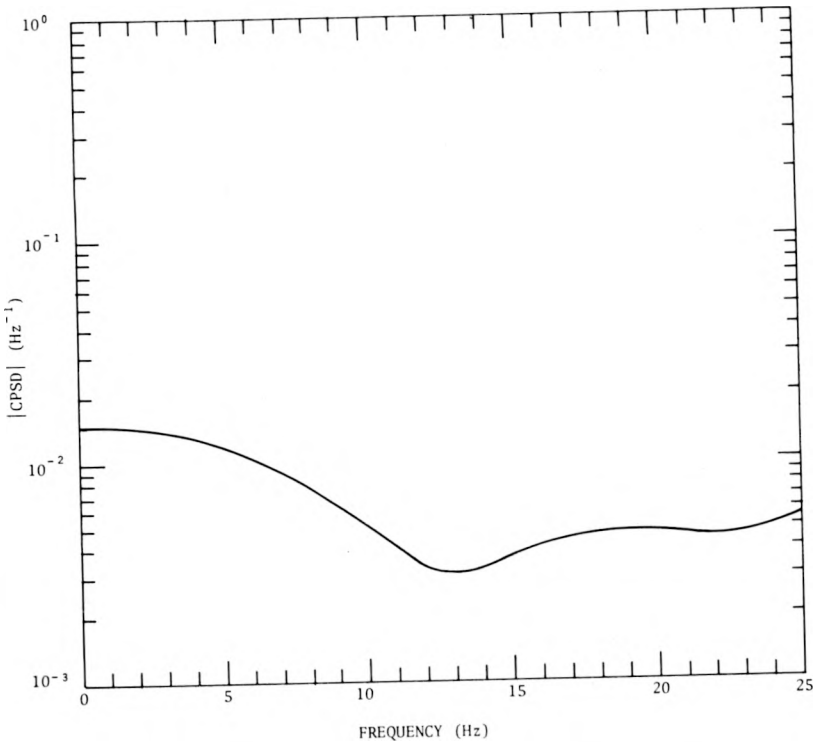

Fig. 1. Predicted cross-power spectral density between void fluctuations at 18- and 54-in. locations.

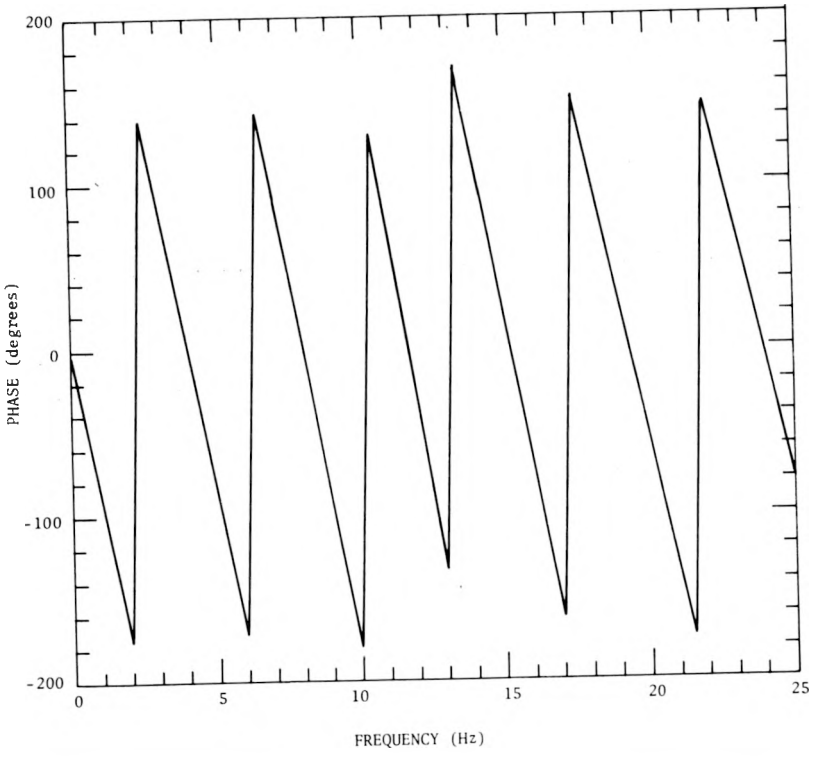

Fig. 2. Predicted phase between void fluctuations at 18- and 54-in. locations.

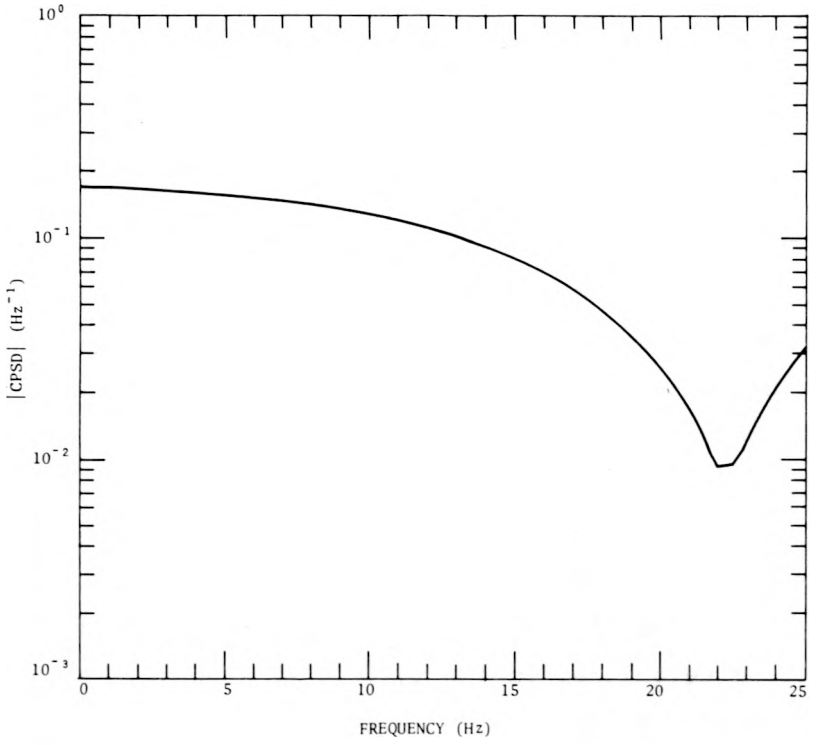

Fig. 3. Predicted cross-power spectral density between void fluctuations at 90- and 126-in. locations.

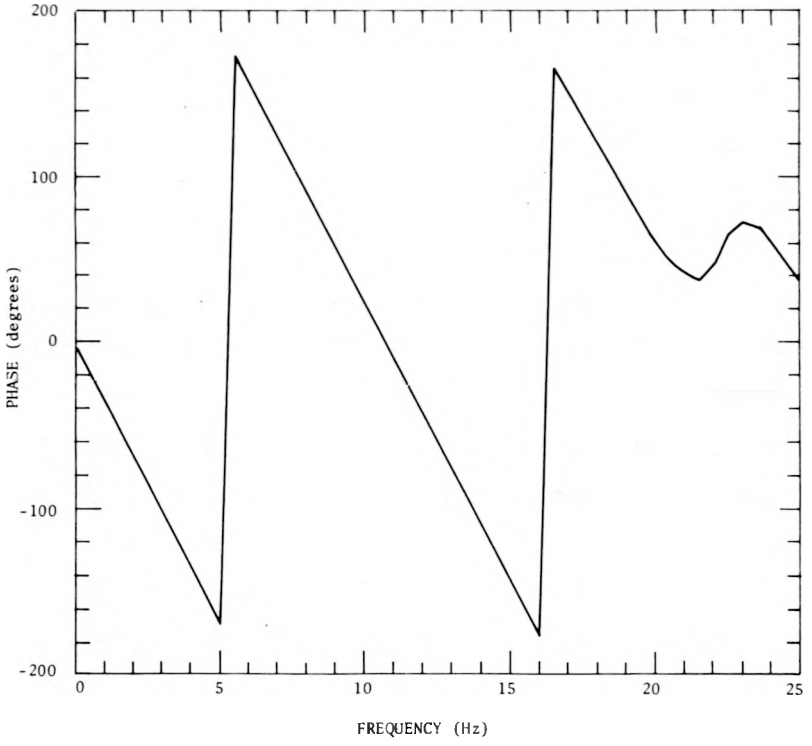

Fig. 4. Predicted phase between void fluctuations at 90- and 126-in. locations.

thereby repudiating the assumed axial correlation of the driving functions.

2.4 Tentative Conclusions from Analytical Investigations

1. An analytical two-phase flow model that neglects "slip" effects yields results that are consistent with experiment when the correct driving noise source characteristics are assumed.
2. The driving noise sources for void fraction fluctuations in a BWR appear to be more nearly uncorrelated than correlated in the axial direction.
3. A summation of the predicted outputs from multiple boiling subchannels yields linearly increasing (absolute value) phases from 0 to 25 Hz; the implied steam velocities are weighted averages of the steam velocities in the individual subchannels.
4. A spatial transfer function or variational technique is required to predict correctly the effects of void fraction fluctuations on the neutron detector response.
5. Simple two-phase flow experiments might be analyzed with the same techniques used in this investigation. A parameter which must be known is the degree of spatial correlation among the various driving noise sources.

2.5 References

1. R. C. Kryter, *Noise Diagnostics for Safety Assessment Quarterly Progress Report for January-March 1977*, ORNL/NUREG/TM-112 (June 1977).
2. P. Gebureck, O. Singh, and D. Stegemann, "Experimental and Theoretical Noise Analysis Investigations in Boiling Water Reactors," *Progress in Nuclear Energy*, 1(2-4), 187-203 (1977).
3. T. Nomura, "Noise Analysis of Boiling Water Reactors," *Proceedings of Japan-U.S. Seminar on Nuclear Reactor Noise Analysis, Tokyo and Kyoto*, 1968.
4. M. M. R. Williams, *Random Processes in Nuclear Reactors*, Pergammon Press (1974).

5. A. Z. Akcasu, *Theoretical Feedback Analysis in Boiling Water Reactors*, ANL-6221 (1960).
6. A. Atta and W. T. King, "Determination of Void Velocities Through Neutron Noise Analysis," to be published in *Nuclear Science and Engineering*.

3. SCREENING TECHNIQUES FOR VIBRATIONAL QUALIFICATION OF NUCLEAR PLANT PIPING

J. E. Stoneking, R. C. Kryter

Purpose. Assess the accuracy of the simplified piping system qualification methods being developed by the ASME Subcommittee on Vibration Monitoring.

Method. Stress analysis of realistic piping systems with the widely used SAP-VA finite element computer code.

First Applications. Liquid natural gas piping system; PWR auxiliary feedwater main steam supply piping.

Follow-On. Effects of pipe contents, insulation, concentrated masses, "soft" restraints.

3.1 Introduction

The ASME Subcommittee on Vibration Monitoring is currently developing simplified qualification methods (screening techniques) by which nuclear plant piping systems undergoing both continuous and transient vibration can be assured safe in terms of maximum internal stress levels, thus meeting the requirements of Section 50.34 of 10 CFR Part 50, the USNRC Standard Review Plan, and similar documents. To keep the qualification methods both simple and applicable to a wide range of piping geometric configurations, many simplifying assumptions and engineering approximations have been incorporated, and these cast doubt on the accuracy of the results and on the validity of the acceptance criteria based on them. Since full-scale experimental verification would be expensive, we have used finite element modeling for initial guidance regarding the adequacy of the simplified qualification methods being considered by the subcommittee.

The simplified method[1] proposed by the subcommittee was developed from basic beam theory, with certain modifications to allow for stress intensification factors, lumped masses, pipe internal contents, and external insulation. There is little doubt that the resultant limiting velocity and displacement criteria would assure the safe performance of a piping system that can be modeled realistically as a simple beam; indeed, conservatism (stress *over*prediction) is almost guaranteed. However, the degree to which geometrically complex nuclear plant piping systems can be considered to be noninterconnected collections of simple beams is, to our knowledge, undemonstrated. To determine the accuracy of this basic assumption of the subcommittee approach, we analyzed three representative piping systems with the SAP-V finite element computer code[2] and thereby generated results against which to judge the accuracy and limitations of the proposed simplified method.

The following procedure was used:

1. We assumed, for lack of a known driving function, that the piping system vibrates in one of its natural modes. We then performed a *dynamic* analysis with SAP-V to determine the first few natural frequencies (eigenvalues) and corresponding mode shapes (eigenfunctions) of the subsystem under investigation.
2. On a mode-by-mode basis, we performed a *static* analysis of the deformed subsystem, i.e., we forced the piping to deform into the desired mode shape and then computed the location and numerical value of the maximum computed stress,* S^c_{max}, introduced by this normalized modal deflection pattern.
3. We calculated the maximum bending stress, S^p_{max}, predicted by the ASME simplified method. The formula used was

$$S^p_{max} = \frac{V_{max}\ i\ 1000}{C_1\ C_2},$$

*This will probably be a bending stress, but SAP-V calculates torsional and axial stresses, as well, to affirm the assumption that the latter can be safely ignored.

where S^P_{max} is the maximum predicted bending stress (psi), V_{max} is the maximum velocity for the mode under study (in./sec), and i, C_1, and C_2 are geometric parameters defined in Sect. 5.4 of Ref. 1 that make allowance for individual subsystem properties.

4. We compared the maximum stresses computed in steps 2 and 3. We defined a stress comparison factor,

$$f \equiv S^P_{max}/S^C_{max} ,$$

for this purpose. We emphasize that the *absolute* stresses computed by either method are not necessarily meaningful, since the maximum amplitude of the modal deflection was specified arbitrarily as 1.2 in.

3.2 Examples

All three examples studied are real piping subsystems: the first two are liquefied natural gas applications, and the third is a major portion of the auxiliary feedwater system for the Watts Bar Nuclear Plant,* an 1177 MWe Westinghouse PWR.

3.2.1 Example I

Figure 5 shows the undeformed shape of piping Example I in isometric view, including the location and type of support constraints. The entire system is constructed of 8-in., Schedule 40 (8" S40) stainless steel pipe. Figure 6 shows the first mode shape; its natural frequency was computed to be 8.92 Hz. A static stress analysis was performed for this first mode with an assumed maximum displacement of 1.2 in., which scaled both the maximum velocity and the maximum stress associated with this mode. The maximum bending (flexural) stress in the system was computed by SAP-V to be 10,600 psi; its location is indicated in Fig. 6. Calculated axial and shear stresses were negligible relative to the bending

---

*System drawing (Fig. 9) courtesy of J.S.G. Williams, the Tennessee Valley Authority, Knoxville, TN.

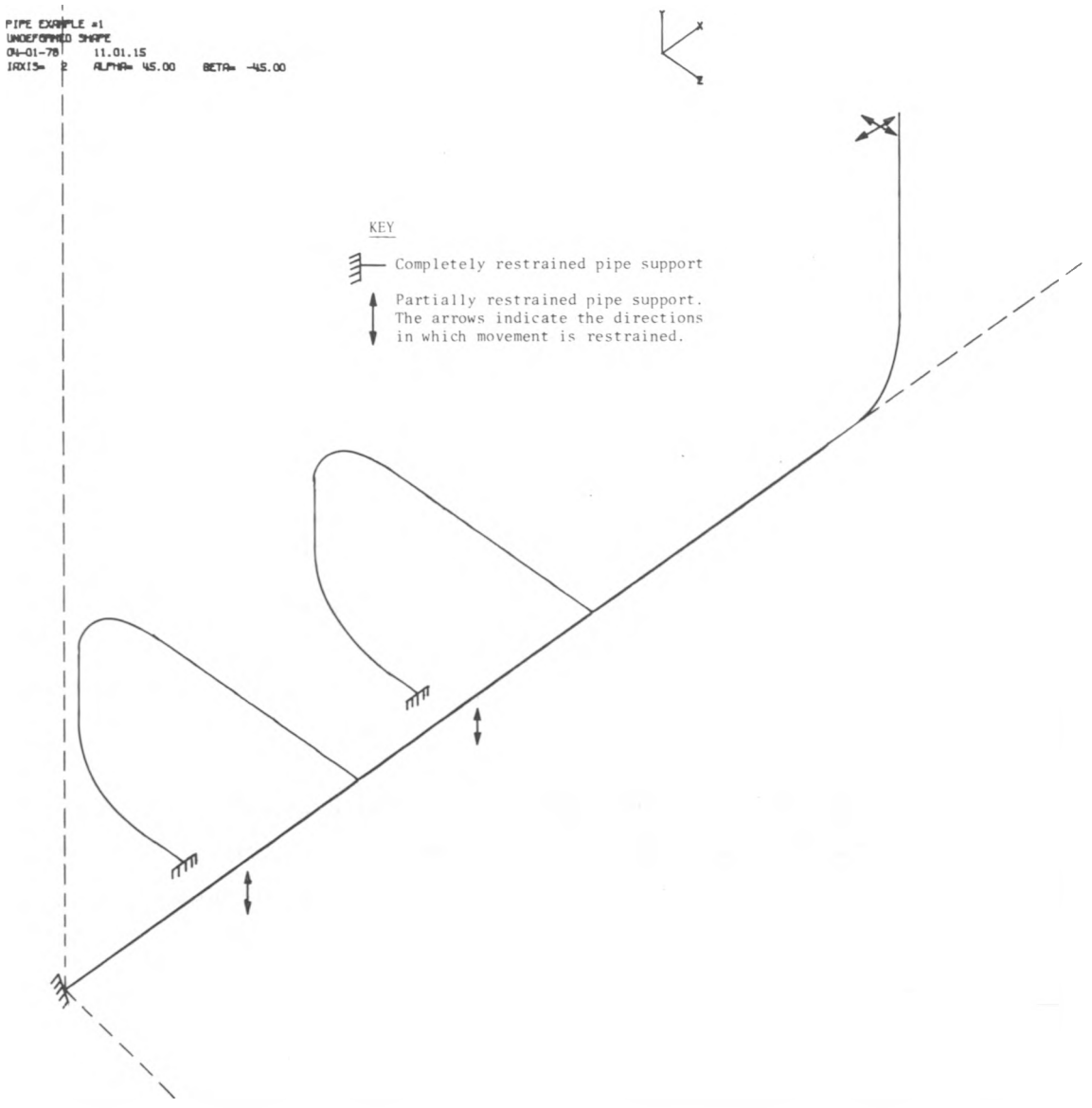

Fig. 5. Piping example I -- undeformed shape.

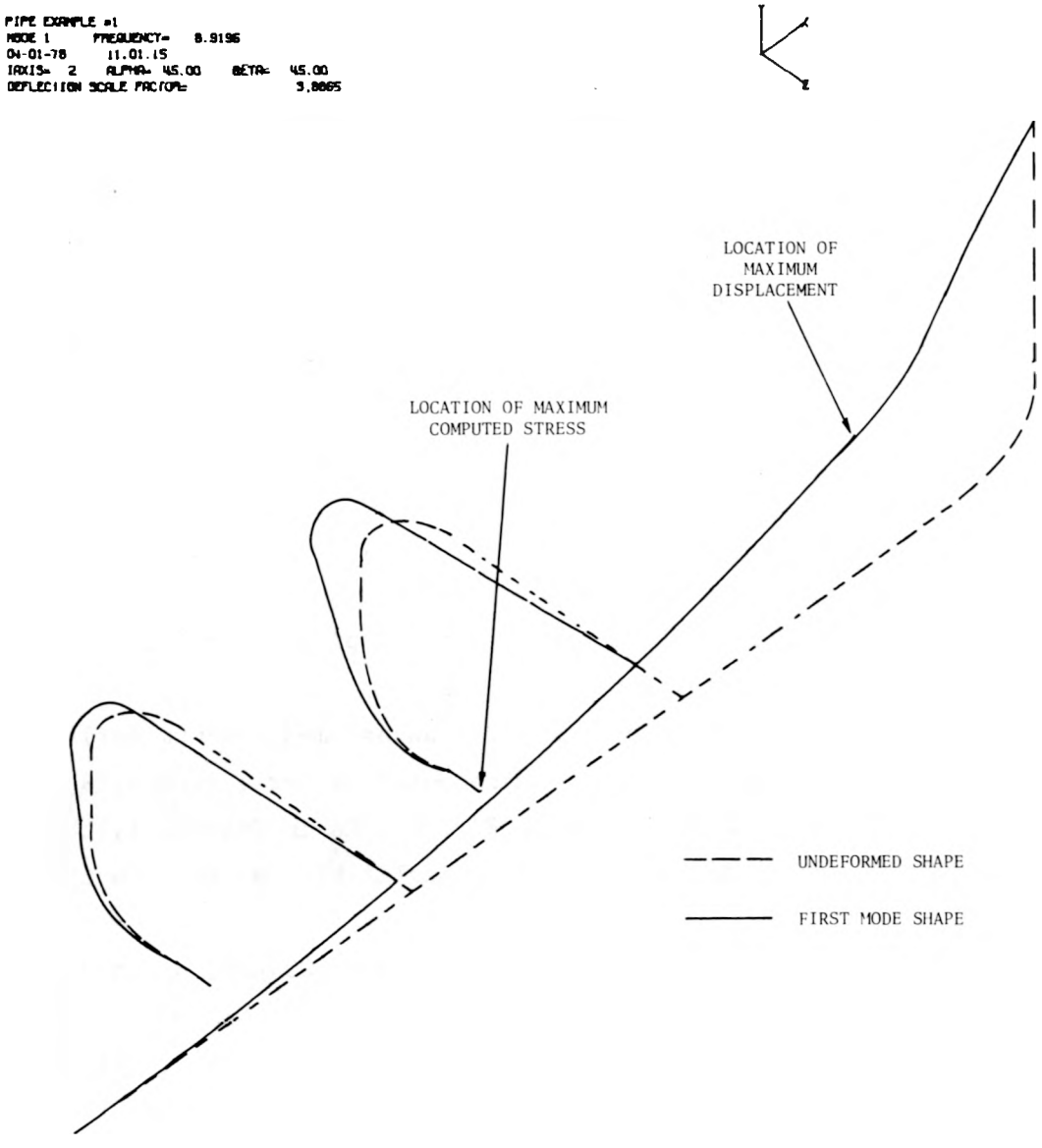

Fig. 6. Piping example I -- first mode shape.

component, a result which supports their neglect in the ASME simplified approach.

The maximum predicted bending stress, S^P_{max}, was computed as 342,000 psi, using the values

$V_{max} = 2\Pi f_1 A_{max} = 67.3$ in./sec,

$i = 5.08$ (stress intensification for a tee), and

$C_1 = C_2 = 1$ (no concentrated masses; empty pipe without insulation)

in the simplified formula (f_1 is the first-mode natural frequency, and A_{max} is the maximum displacement throughout the subsystem). The stress comparison factor for Example I is thus $f_I \approx 32$; that is, the ASME simplified formula greatly *over*predicts the bending stresses in this Example and is therefore highly conservative for qualification purposes.

3.2.2 Example II

Figures 7 and 8 depict the undeformed subsystem for piping Example II and its first mode shape, respectively. As in Example I, the entire system is constructed of 8" S40 stainless steel pipe. The fundamental natural frequency was computed to be 19.7 Hz.

The static analysis was performed for an assumed maximum deflection of 1.2 in., and this yielded a maximum computed flexural stress, S^c_{max}, of 35,300 psi at the location shown in Fig. 8. As in Example I, the axial and shear components of stress were negligible relative to the bending component.

From the ASME simplified method, S^P_{max} is 208,000 psi, using $V_{max} = 148.5$ in./sec, $i = 1.40$ (stress intensification for an elbow), and $C_1 = C_2 = 1$. The stress comparison factor is therefore $f_{II} \approx 5.9$, which is clearly conservative but not by so large a margin as in Example I.

3.2.3 Example III

The considerably more complex piping subsystem analyzed as Example III is shown first in Fig. 9 as an isometric engineering drawing and then in Fig. 10 as modeled for SAP-V. The piping is mostly 4" S80, but sizes vary from 3/4" S80 to 10" S40, and there are many directional

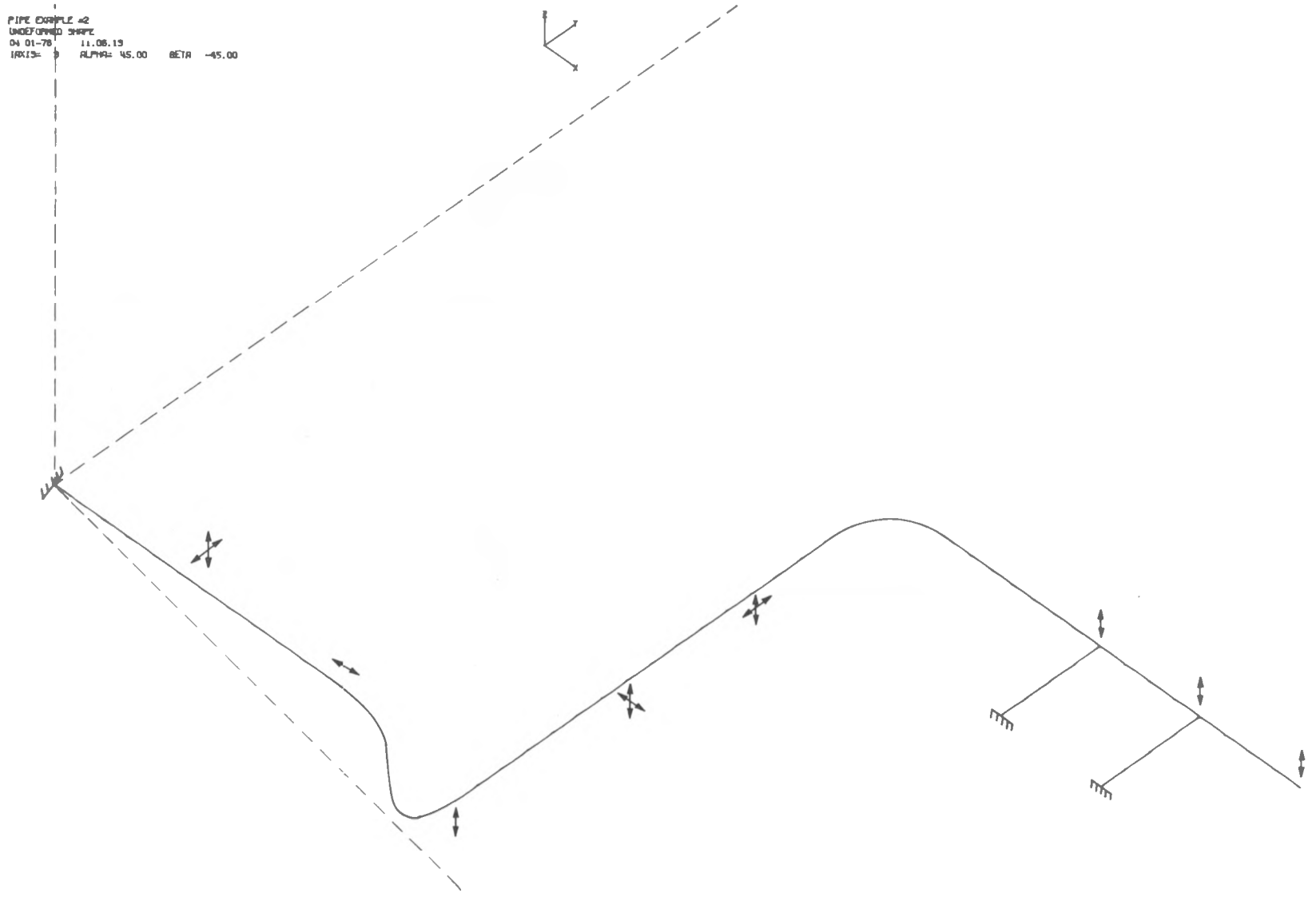

Fig. 7. Piping example II -- undeformed shape.

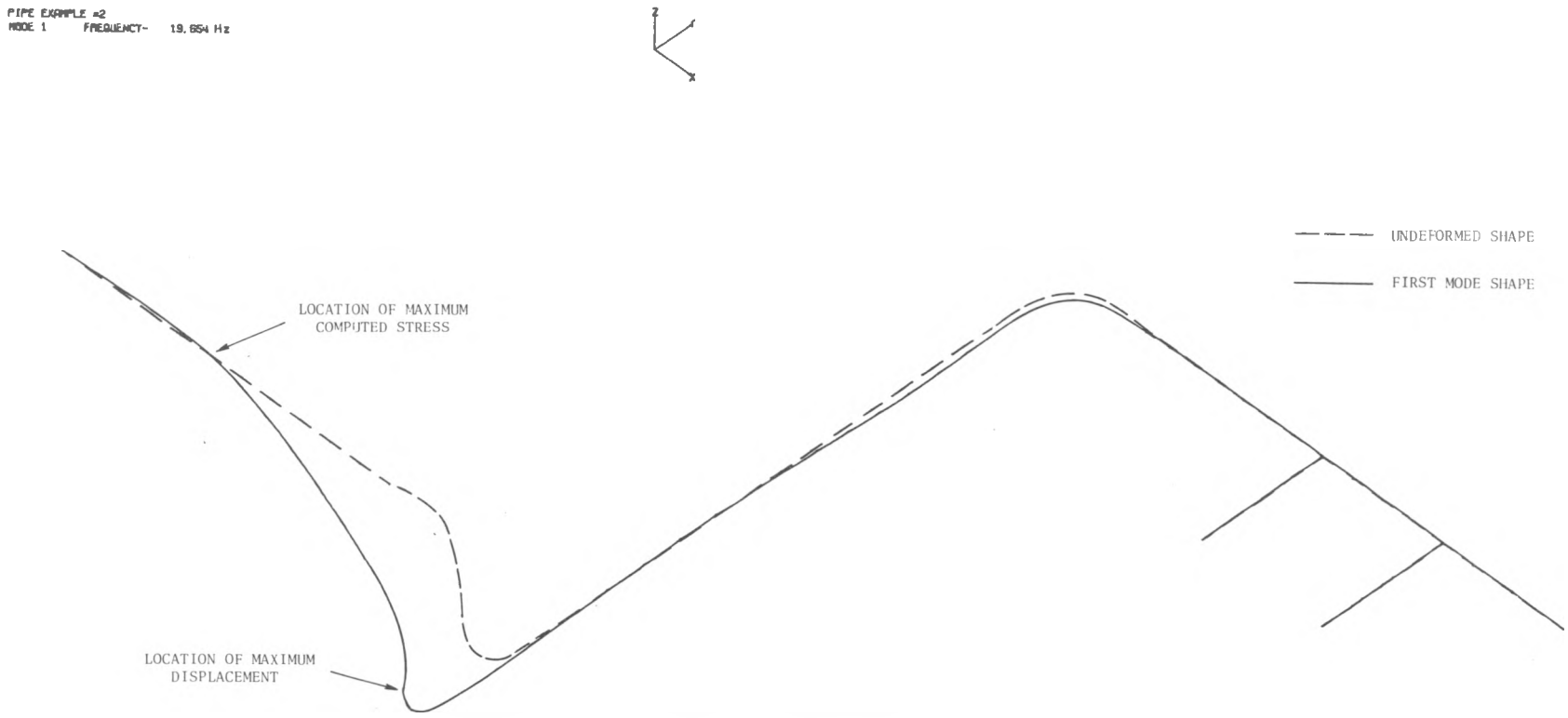

Fig. 8. Piping example II -- first mode shape.

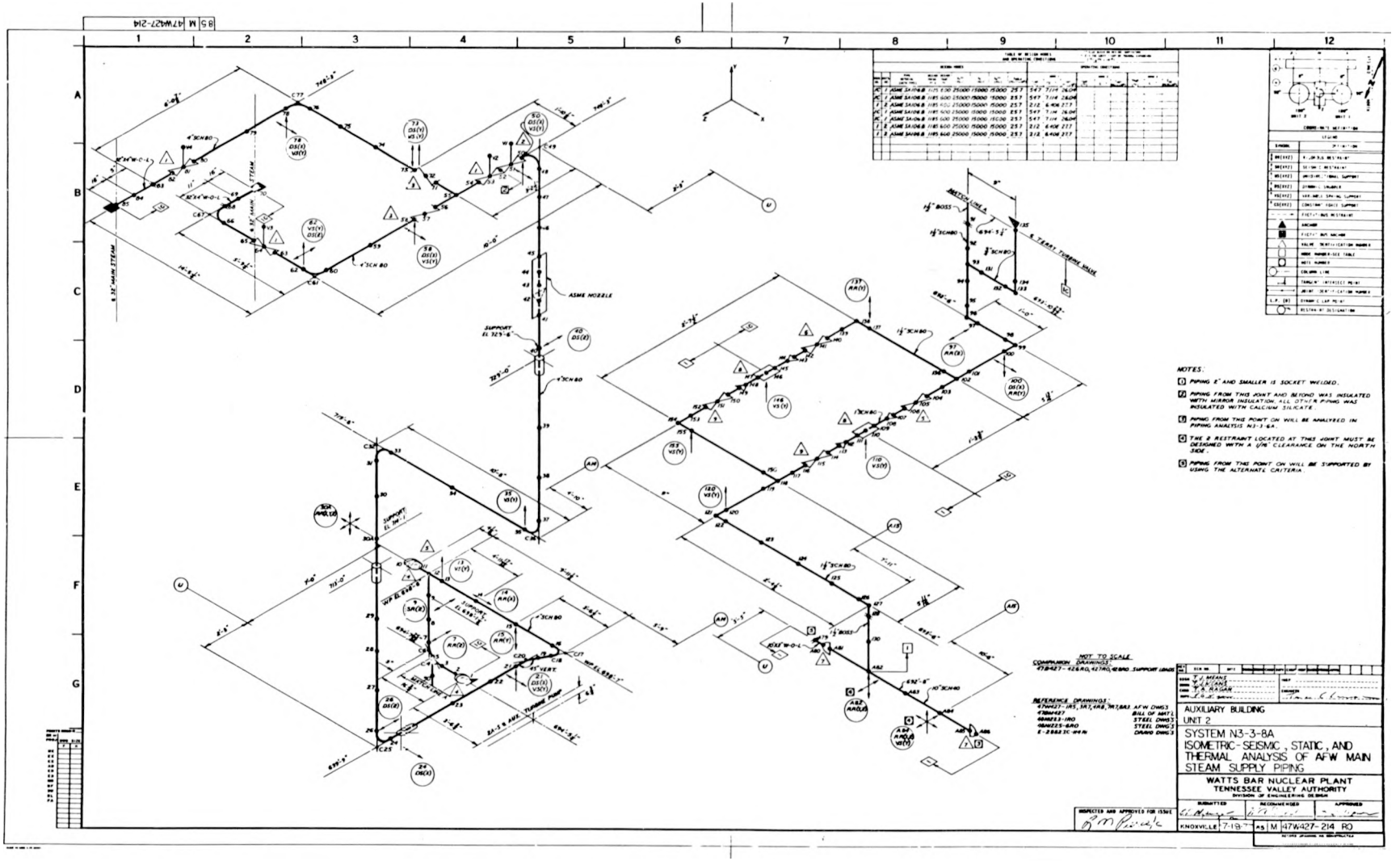

Fig. 9. Piping example III -- isometric system drawing.

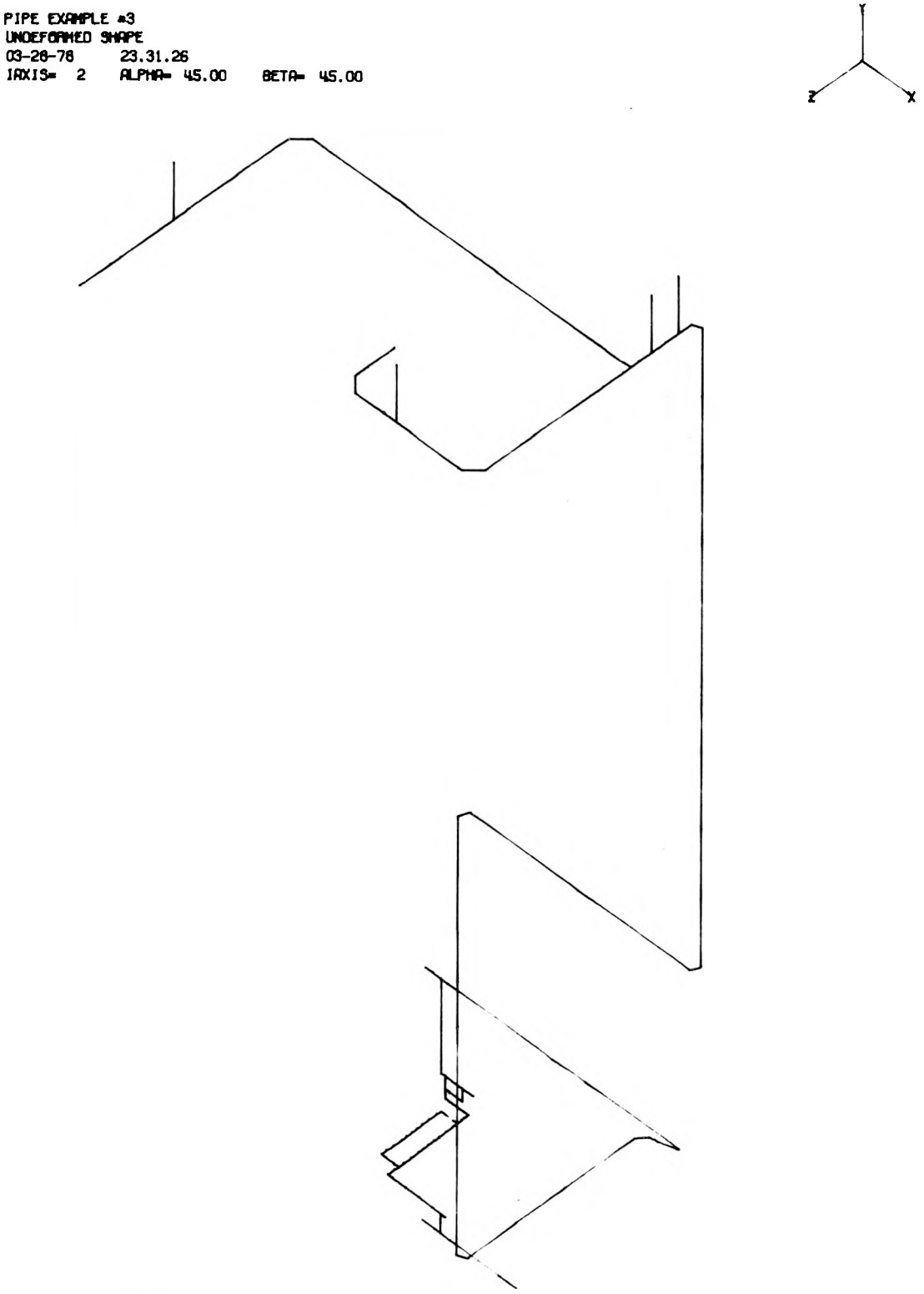

Fig. 10. Piping example III -- computer model of system shown in Fig. 9.

restraint mechanisms and concentrated masses (valves). This example provides a good test for the basic assumption underlying the ASME subcommittee's simplified formula, viz., that a complex piping system can be analyzed as if it were a collection of noninterconnected simple subsystems which, in turn, can be approximated by simple beams. For this Example, the computed and predicted stresses were compared for both the first and second natural modes of vibration, which are shown in Figs. 11 and 12.

3.2.3.1 First mode. The lowest computed natural frequency was 3.87 Hz; a static analysis was performed for a maximum modal displacement of 1.2 in. The locations of both this maximum displacement (which, by definition in a single-mode system, is also the location of maximum velocity) and of the resulting maximum bending stress are indicated in Fig. 11. The computed value for S^{c}_{max} was 9500 psi, and since the axial and shear stresses were relatively small, they were ignored. The predicted stress S^{p}_{max} was 48,400 psi, using V_{max} = 29.2 in./sec, i = 1.66 (stress intensification for an elbow), and $C_1 = C_2 = 1$. The ratio of the predicted and calculated stresses for Example III, mode 1, is thus $f^{(1)}_{III} \approx 5.1$, a value which agrees well with the value of 5.9 in Example II.

3.2.3.2 Second mode. The second natural frequency was computed to be 4.01 Hz. Although the frequency separation from the fundamental is small, the mode shapes are quite different (compare Fig. 11 with Fig. 12). A static stress analysis was again performed, using a maximum modal displacement of 1.2 in. (the location is indicated in Fig. 12). The maximum flexural stress was computed to occur near the point of maximum deflection, but in our opinion this result is invalid, owing to (1) the particular method used to force the piping subsystem into its second natural mode shape, and (2) the artificial manner in which the present model of the piping terminates near this location of maximum stress (the real system, of course, continues beyond this point). Neither of these modeling inadequacies is intrinsic to the analysis method or to the SAP-V code; both can be corrected by relatively simple changes to the piping model, and we expect to do so next quarter.

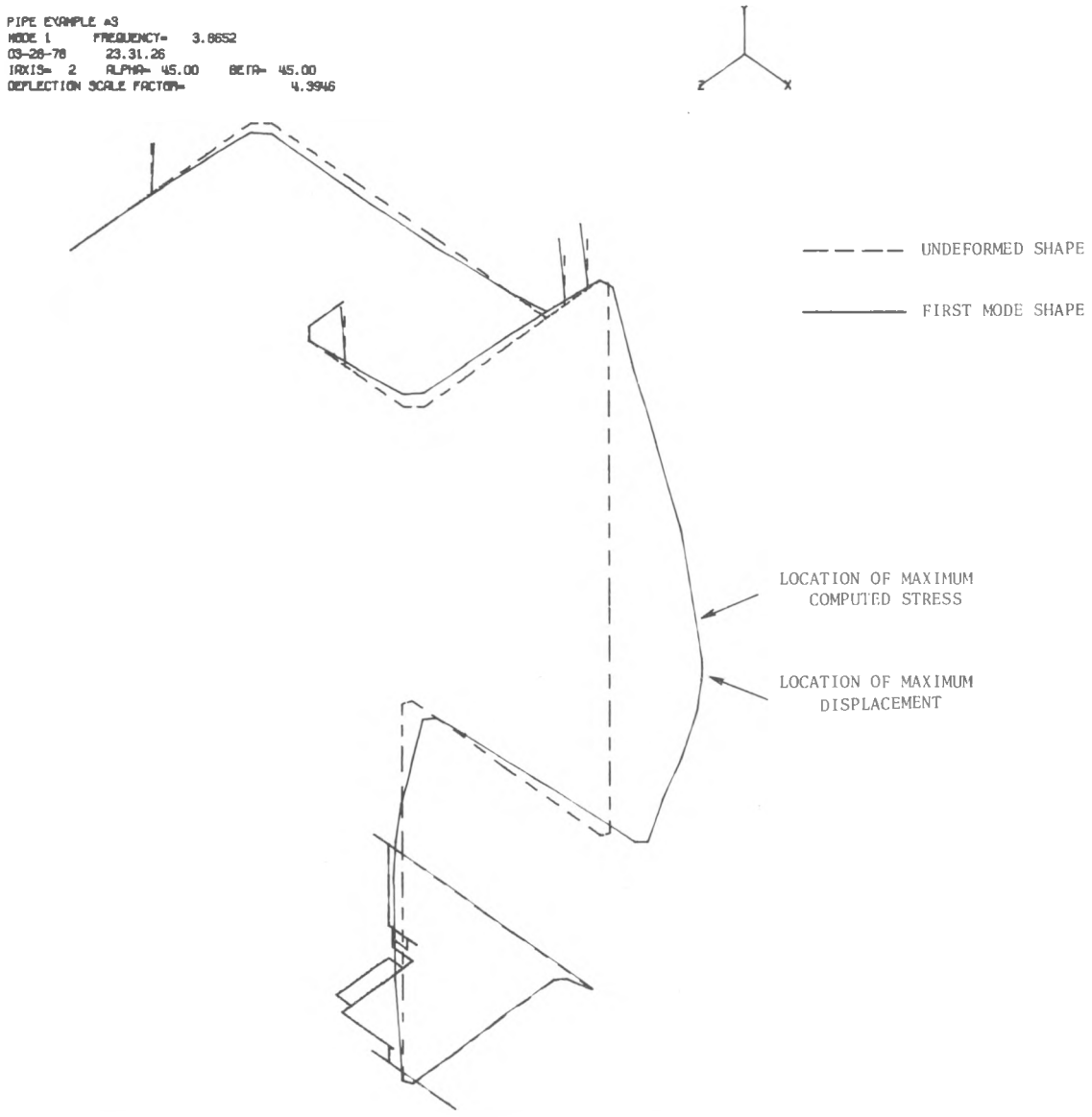

Fig. 11. Piping example III -- first mode shape.

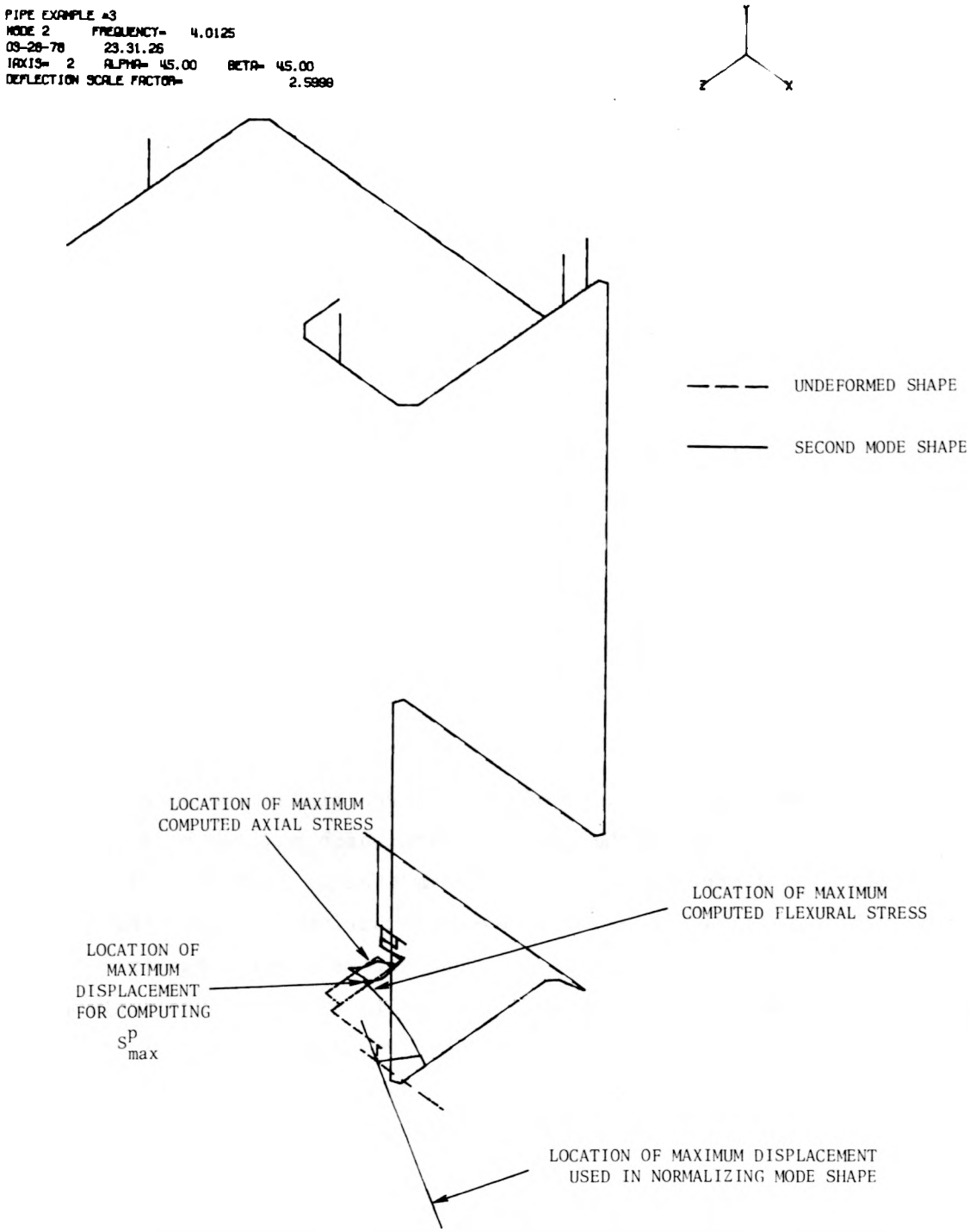

Fig. 12. Piping example III -- second mode shape.

On the supposition that regions of the piping far away from the artificial restraint point imposed by the present modeling might still yield useful results, we examined the second-mode-shape stresses near the position of the *second* largest displacement occurring between supports. A modal displacement of 0.564 in. (about half that of the maximum displacement within the system) had been computed for the position indicated in Fig. 12, and the maximum computed flexural stress* in this same run of pipe was 80,000 psi. However, since this maximum stress occurred at a tee, a further stress intensification factor of 2.14 was required (SAP-V does not account for stress intensification at tees), thus raising S^c_{max} to 171,000 psi. With V_{max} = 14.2 in./sec, i = 2.14, and $C_1 = C_2 = 1$, the simplified method predicted a maximum bending stress in this same piping run of S^p_{max} = 30,400 psi, resulting in a stress comparison factor $f^{(2)}_{III} \approx 0.18$ for the Example III, second-mode vibrations. This result implies that the ASME simplified method *under*predicts the bending stress under these circumstances by a factor of 5.6, but we do not consider such a conclusion valid, owing to the modeling inadequacies described previously.

3.3 Interim Conclusions

The results from our study of these three piping system examples show a large variation in the accuracy with which maximum bending stresses are predicted by the ASME subcommittee's simplified piping qualification method. However, in every comparison but one (the validity of which must be questioned) the stress predictions from the simplified method erred in a safe direction for piping qualification purposes. Additional test cases, perhaps even corroboration from experimental data acquired on real piping systems, will be necessary to establish the universality and general magnitude of this apparent conservatism.

---

*Axial and shear stresses were negligible at this location of maximum flexural stress, but at a nearby location SAP-V computed a very high axial stress (280,000 psi). Since flexural stresses were predominant in all other cases calculated, this result warrants further study.

3.4 Future Work

In the next quarter, we plan to (1) correct the Example III, second-mode calculations by extending the physical boundaries of the subsystem modeled and by modifying the manner in which the piping is forced to conform to its second mode shape, and (2) investigate the applicability of the simplified method in the presence of additional complicating effects, such as vibrations dominated by concentrated masses ($C_1 \neq 1$) and insulated, fluid-filled pipes ($C_2 \neq 1$).

3.5 References

1. The simplified method is described in the notes of the Subcommittee Task Group 5.0 August 17, 1977, meeting in San Francisco, CA.
2. Bathe, Wilson, and Peterson, "SAP-VA -- A Structural Analysis Program for Static and Dynamic Response of Linear Systems," University of California at Berkeley (1973).

4. CHANGES IN BWR-4 IN-CORE NEUTRON NOISE RESULTING FROM DRILLING HOLES IN LOWER TIE PLATES

D. N. Fry, W. T. King, E. L. Machado

Purpose. Investigate the changes in neutron noise associated with the introduction of drilled fuel bundle tie plates in BWR-4s.

Method. Comparison of frequency spectra of recorded in-core neutron noise data from one plant having drilled tie plates and from three plants having undrilled tie plates.

4.1 Introduction

In-core neutron noise data from local power range monitor (LPRM) detectors recorded previously at four BWR-4 reactors were processed further during this quarter, using Fourier analysis. This data processing is the first step in our investigation of the changes in neutron noise spectra that are apparently related to the use of drilled tie plates, a modification which was introduced to eliminate impacting of instrument tubes against adjacent fuel channel boxes. Table 1 lists

Table 1. Status of BWR-4 plants when neutron noise was recorded

Plant	Power (MWe)/ % Flow	No. of LPRM Strings in Core	No. of Fuel Pins per Bundle	Bypass Flow Modification
I	1059/100%	43	49	Plugged support plate
II	1080/97%	43	49	Plugged support plate
III	1092/97%	43	63	Drilled tie plates
IV	640/81%	31	49	Plugged support plate

the plant power and flow at the time of data recording, the number of fuel pins per bundle, and the status of bypass flow modification. (In Plants I, II, and IV the preexistent bypass cooling holes were plugged, but no new holes were drilled in the fuel bundle lower tie plates.)

4.2 Data Reduction Program

Neutron noise signatures were obtained from the data recordings with the aid of a computer program developed especially for simultaneous analysis of signals from the four neutron detectors (ordered A, B, C, D, from bottom to top of core, respectively) located in each LPRM instrument tube. The analysis program computed auto-power spectral densities (APSD) of the individual detectors and the various cross-power spectral densities (CPSD), coherence, and phase relationships between the detectors. These noise signatures were stored on computer disks so that they can be recalled and compared with results from different plants.

4.3 Comparison of Results

Composite signature plots (Figs. 13a-d) obtained previously showed that the coherences in the 1-10 Hz frequency region between the upper two detectors (C and D) were significantly greater for Plant III (Fig. 13c), which has drilled tie plates, than for the others. However, we

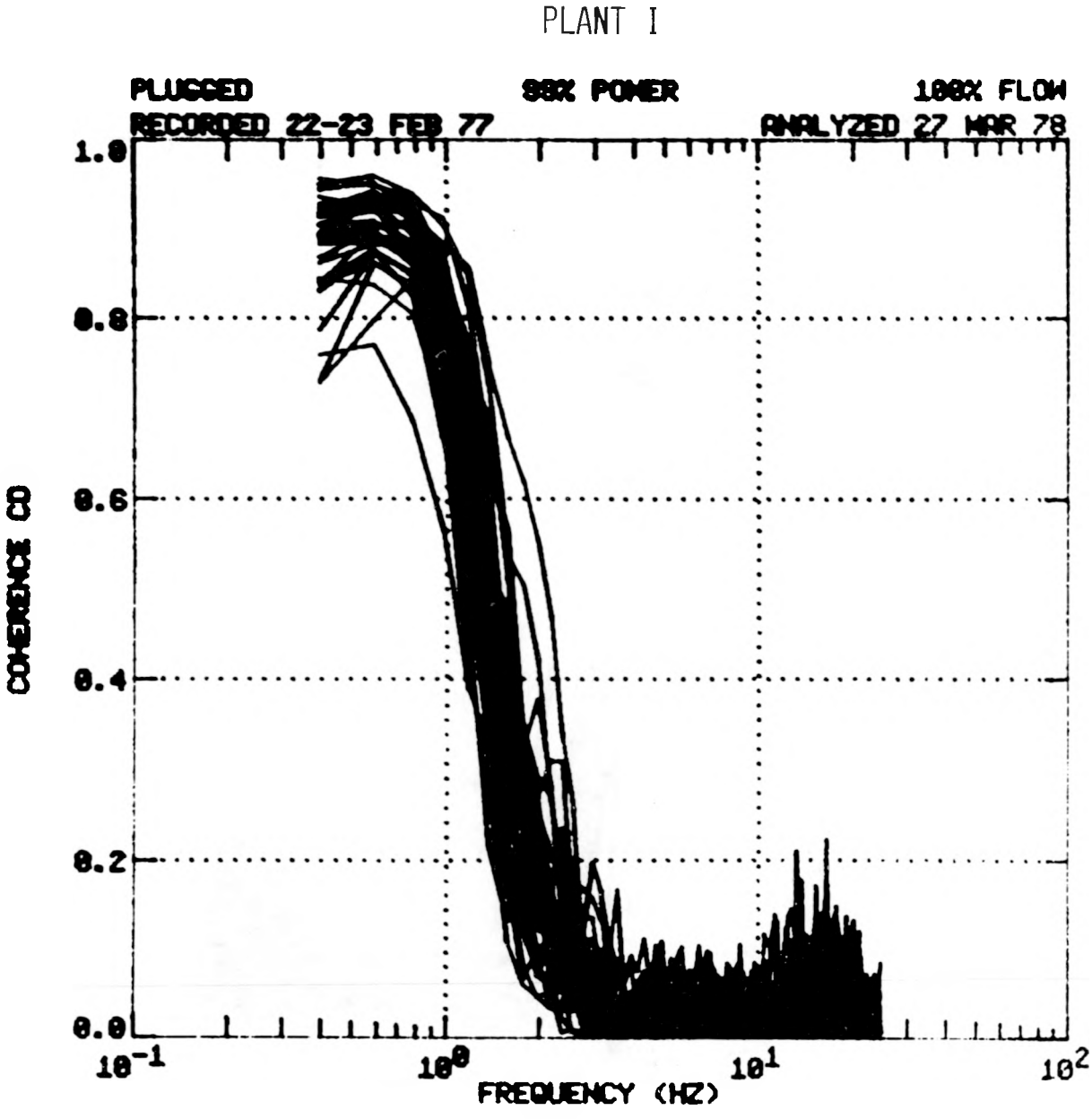

Fig. 13a. Coherence between C and D LPRM detectors in Plant I.

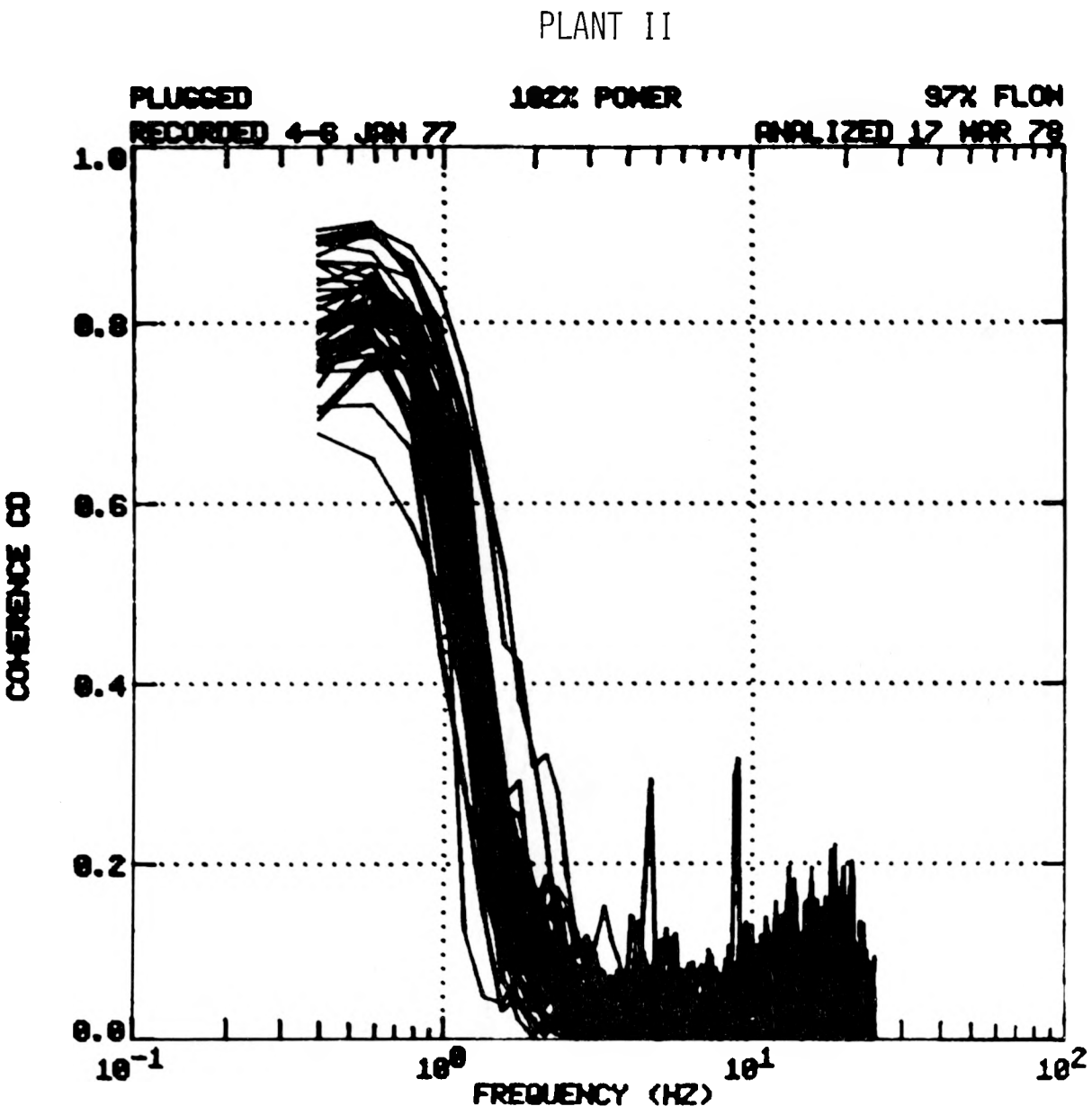

Fig. 13b. Coherence between C and D LPRM detectors in Plant II.

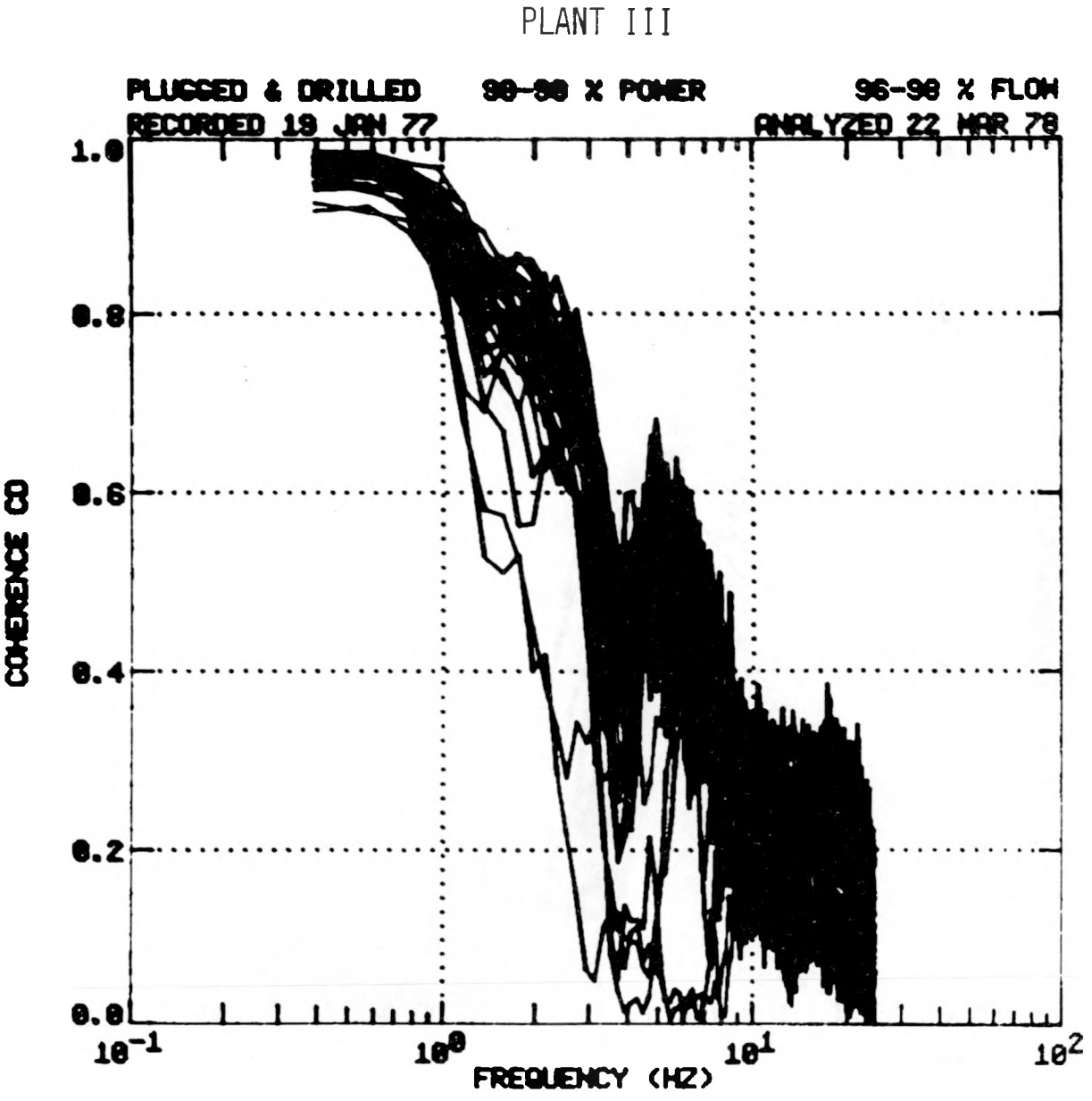

Fig. 13c. Coherence between C and D LPRM detectors in Plant III.

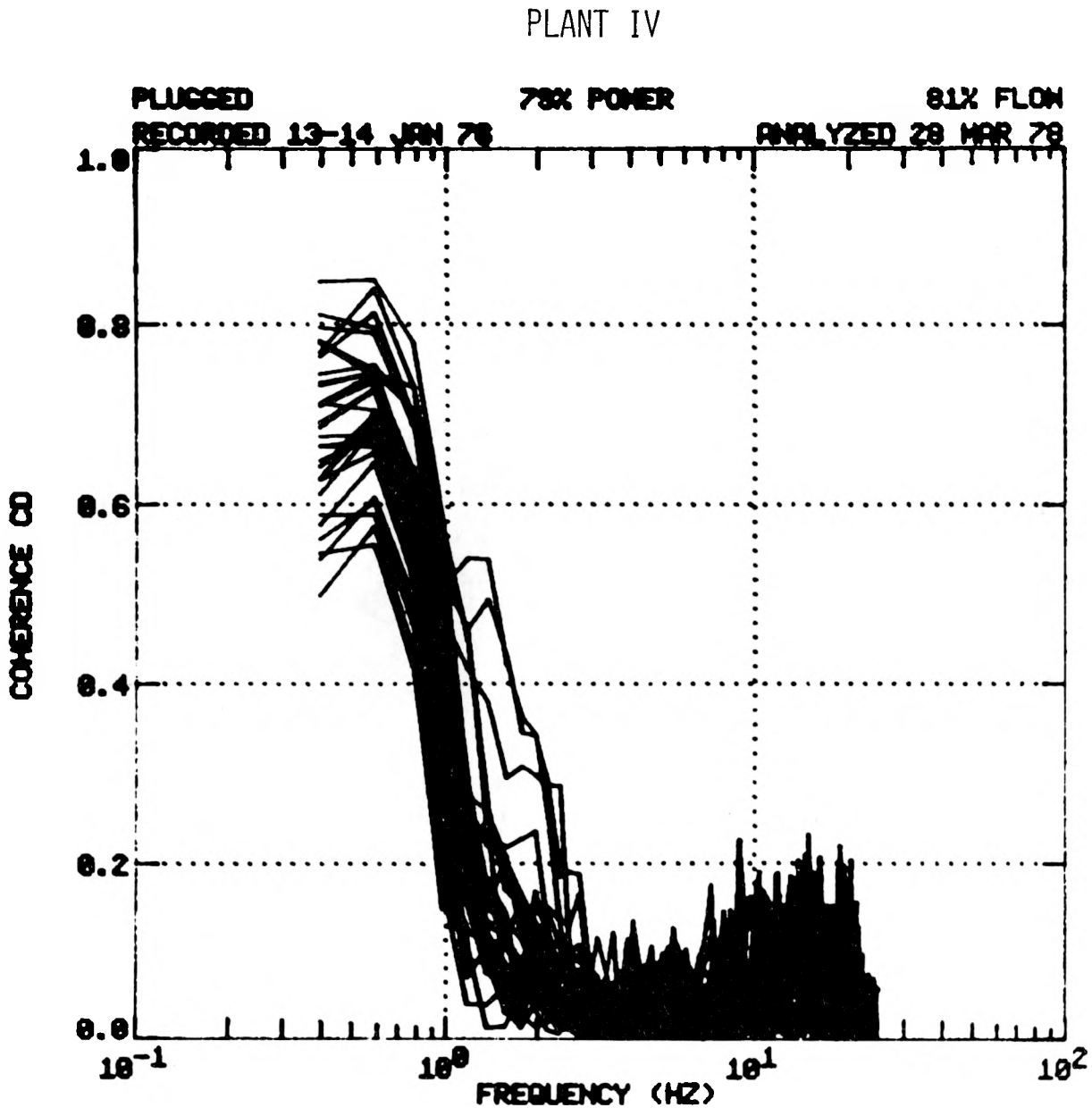

Fig. 13d. Coherence between C and D LPRM detectors in Plant IV.

cannot rule out the possibility that these greater coherences may be due to Plant III having 63 fuel pins in each fuel bundle, whereas the others have 49. Figure 13c also shows that a few core locations of Plant III have coherence signatures that are similar to those from the other plants.

We attempted to determine which LPRM signatures were similar by plotting the data in a different manner. For example, Fig. 14 depicts the magnitude of the average coherence between the C and D detectors in Plant III in the 4-5 Hz frequency band as a function of LPRM position (on this plot, the symbol "B" at an LPRM position indicates that either the C or the D detector was removed from service at the time these data were recorded). At four locations near the core periphery (16-09, 16-57, 48-09, and 56-25), the coherence is low -- similar to that observed in plants without drilled tie plates. We have no explanation for this observation.

The differences in coherence between plants with and without drilled tie plates are most noticeable for the C-D detector pair. Indeed, Fig. 15c shows that the B-C coherences in the plant with drilled tie plates are quite similar to those observed in the other plants. Other plots (not shown) likewise show negligible differences among the A-B coherences of the four plants.

It is premature to speculate on the cause of the differences in C-D coherence and on why the signatures of a few peripheral LPRM strings in the plant having drilled tie plates appear similar to those in the plants having plugged core support plates. Next quarter we will analyze the signatures further and attempt to arrive at an explanation for these observations.

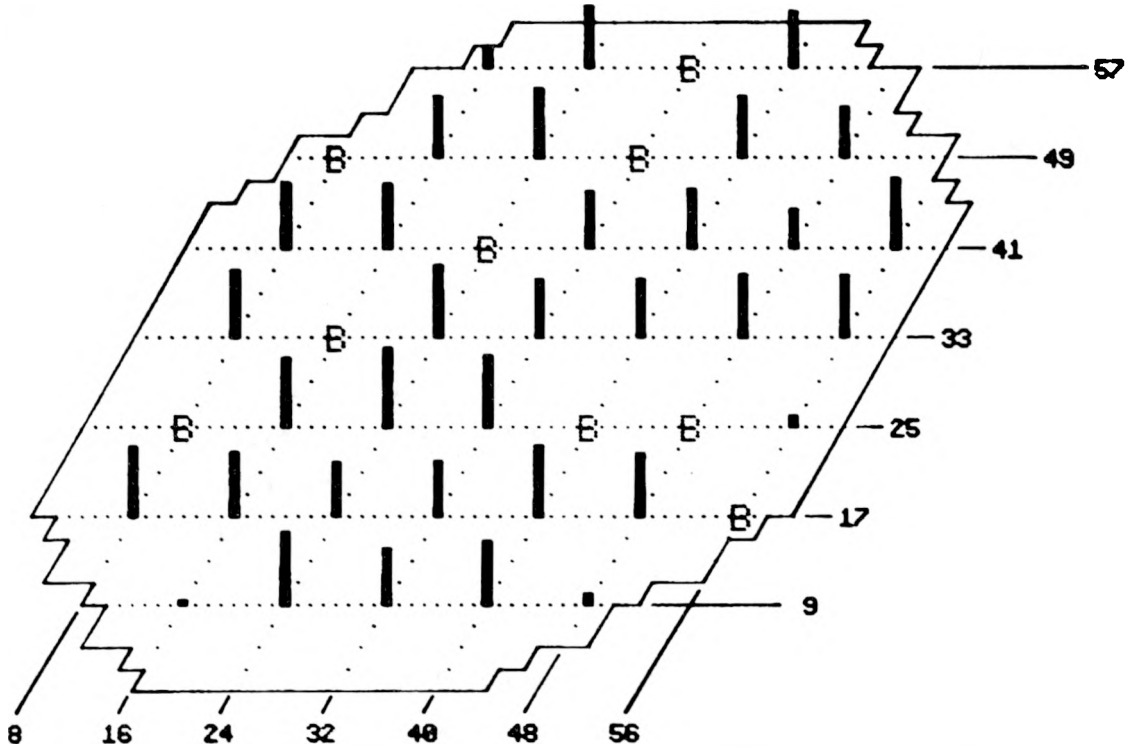

Fig. 14. Coherence between C and D LPRM detectors in the 4-5 Hz band as a function of core position in a plant with drilled fuel (Plant III).

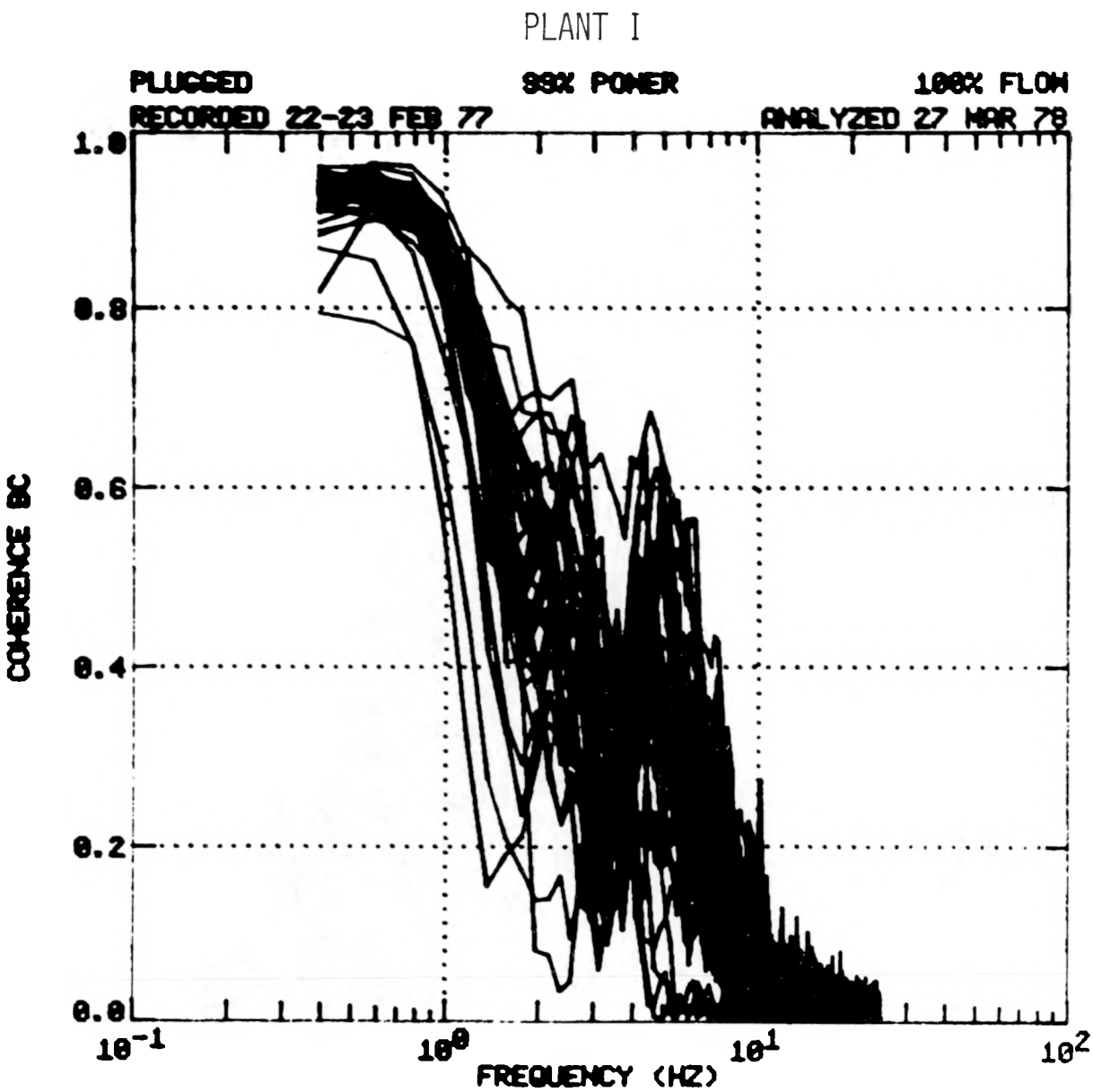

Fig. 15a. Coherence between B and C LPRM detectors in Plant I.

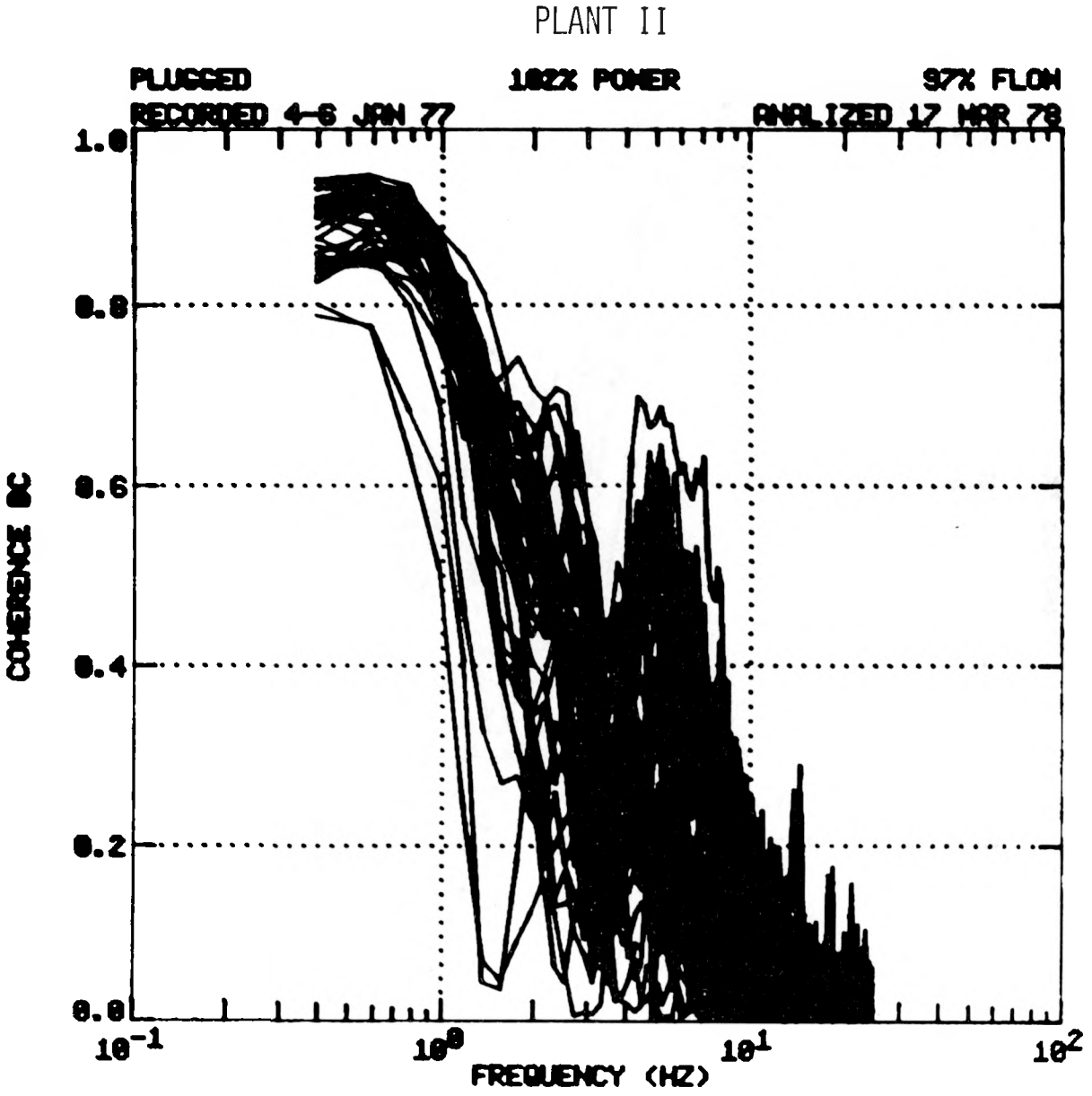

Fig. 15b. Coherence between B and C LPRM detectors in Plant II.

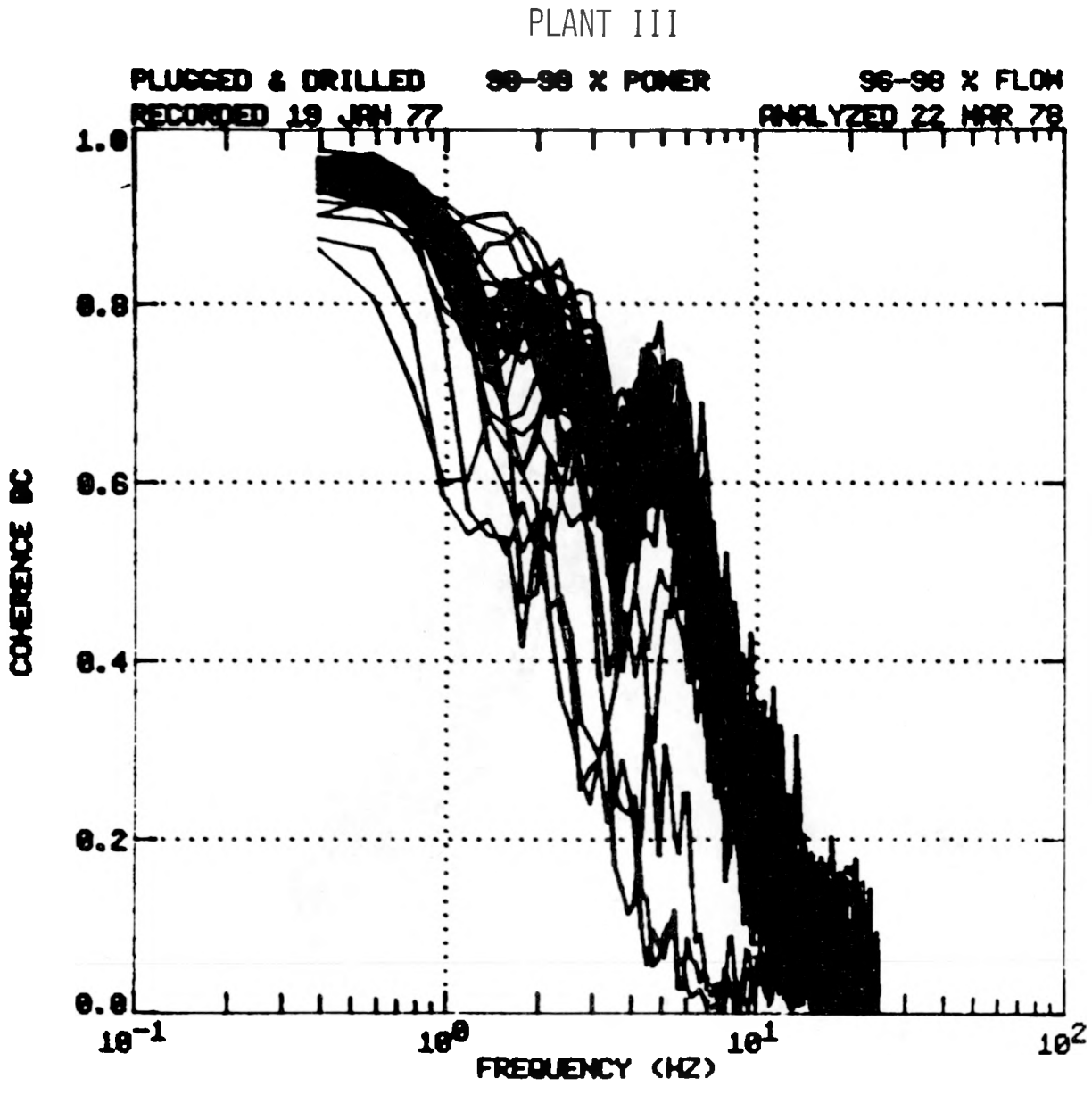

Fig. 15c. Coherence between B and C LPRM detectors in Plant III.

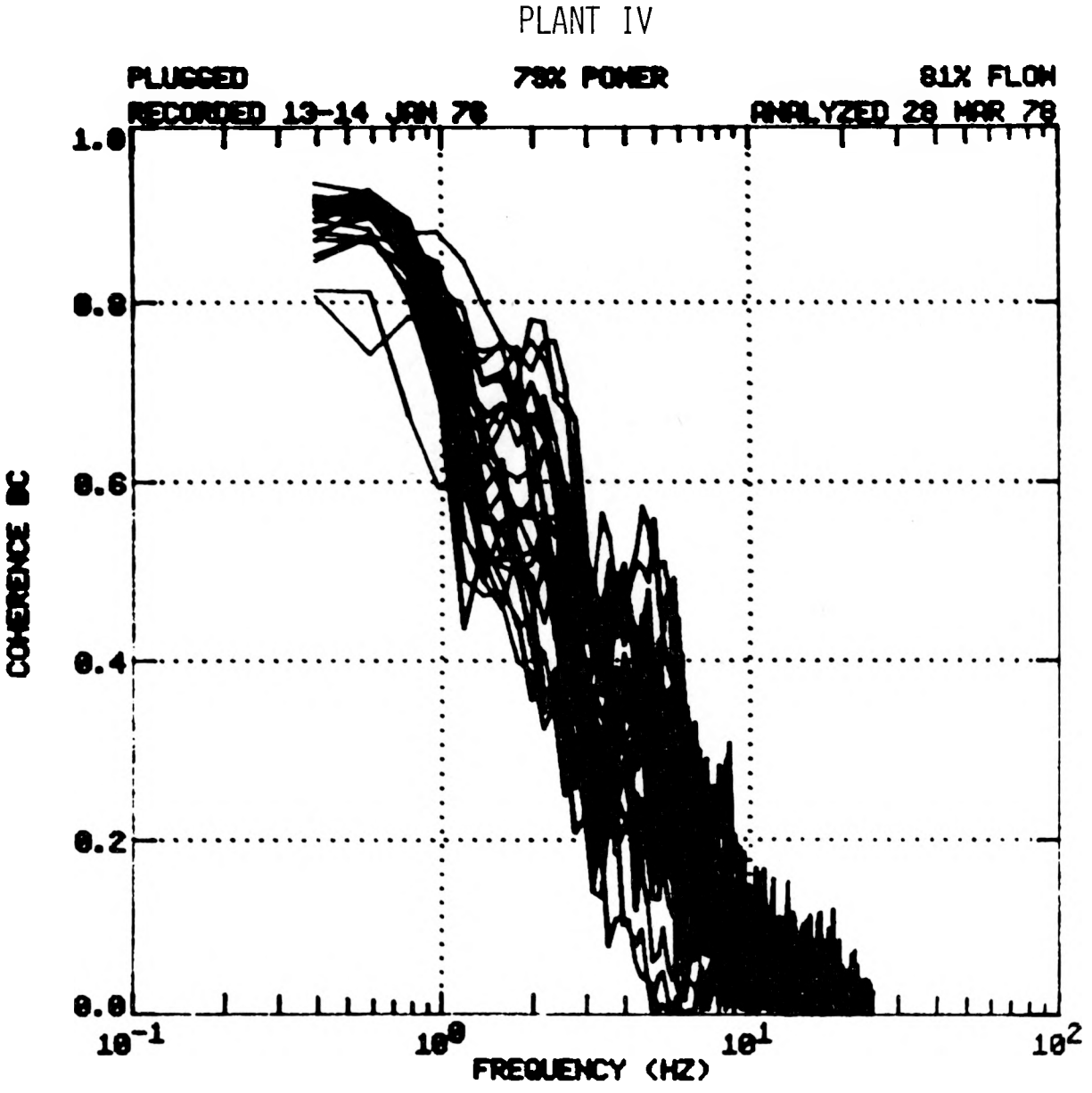

Fig. 15d. Coherence between B and C LPRM detectors in Plant IV.

NUREG/CR-0145
ORNL/NUREG/TM-207
Dist. Category R1

Internal Distribution

1-5. R. S. Booth
6. W. B. Cottrell
7. G. F. Flanagan
8. M. H. Fontana
9. D. N. Fry
10. W. O. Harms
11. H. N. Hill
12. R. C. Kryter
13. F. R. Mynatt
14. F. H. Neill
15. L. C. Oakes
16. H. Postma
17. C. W. Ricker
18. G. S. Sadowski
19-20. Myrtleen Sheldon
21. D. B. Trauger
22. G. D. Whitman
23. Patent Office
24-25. Central Research Library
26. Y-12 Document Reference Section
27-29. Laboratory Records Department
30. Laboratory Records (RC)

External Distribution

31-38. Director, Office of Nuclear Regulatory Research, U.S. Nuclear Regulatory Commission, Washington, DC 20555
39. Director, Reactor Division, DOE, ORO
40. Director, Research and Technical Support Division, DOE, ORO
41. W. S. Farmer, Reactor Safety Research Division, NRC, Washington, DC 20555
42. G. C. Millman, Office of Standards Development, NRC, Washington, DC 20555
43. H. J. Vander Molen, Office of Nuclear Reactor Regulation, NRC, Washington, DC 20555
44. Public Document Room, H-Street, NRC, Washington, DC 20555
45-352. Given distribution as shown in category NRC-1 (25 copies - NTIS)